2015

Catalytic Role of Boron Nitride in the Thermal Decomposition of Ammonium Perchlorate

Kevin Grossman
University of Central Florida

CATALYTIC ROLE OF BORON NITRIDE IN THE THERMAL DECOMPOSITION OF AMMONIUM PERCHLORATE

by

KEVIN GROSSMAN
Bachelor of Science, SUNY, The College at Brockport Brockport, NY 2012

A thesis submitted in partial fulfillment of the requirements
for the degree of Master of Science
in the Department of Material Science and Engineering
in the College of Engineering and Computer Science
at the University of Central Florida
Orlando, Florida

Summer Term
2015

Major Professor: Sudipta Seal

ABSTRACT

The decomposition of Ammonium Perchlorate (AP), a strong oxidizer used in solid rocket propellant, is widely studied in an attempt to increase the burn characteristics of propellants. Many materials have been shown to catalyze its decomposition, but little is known about the mechanism by which AP decomposition becomes catalyzed. In this study, Boron Nitride (BN) nanostructures, a material previously unknown to act as a catalyst, is studied. The decomposition reaction is studied by thermo-gravimetric analysis / differential scanning calorimetry, X-ray photoelectron spectroscopy, fourier transform infrared spectroscopy, transmission electron microscopy and scanning electron microscopy. The goal of this study is to discover the activation energy of this catalyst reaction, intermediary products of the reaction, mechanism of reaction and end state of the boron nitride nanostructures (ie, if the BN acts as a true catalyst, or participates on the overall reaction and has some end state that's different from the initial state). Four variations of BN have been synthesized using a hydrothermal process; BN nanoribbons, Boron Rich BN, Nitrogen-Rich BN, and high surface area BN. It is shown that the decomposition of AP is significantly altered when in the presence of BN and the mechanism through which BN catalyzes the decomposition is most likely the presence of oxidized nitrogen species on the BN material.

I dedicate this work to my parents, who have been a constant source of inspiration and motivation

ACKNOWLEDGMENTS

I would like to thank my faculty advisor, Prof. Sudipta Seal, for his support and motivation during my course of study and research at UCF. I am thankful to the thesis committee members for (Dr. Helge Heinrich and Dr. Kevin Coffey) for providing their valuable time, as well as my fellow researchers at the Advanced Materials Processing and Analysis Center (AMPAC), who have always been willing to lend a helping hand to me. This research has been funded by AMPAC.

TABLE OF CONTENTS

LIST OF FIGURES

LIST OF TABLES

CHAPTER ONE: INTRODUCTION

Solid propellant is an energetic material composed of metal fuel (usually Magnesium[1] or Aluminum[2]) and solid oxidizer bound by a polymer matrix. Along with these basic components, other components are often included into a propellant mixture such as plasticizer, and burn modifying additives. Intense research in this area is warranted by the material's utility in a wide variety of areas such as demolition and space exploration. Solid propellant has several advantages of its liquid counterpart, among which include tunability, shape controllability, storability and chemical and thermal stability. The most commonly used oxidizer used in solid propellant is Ammonium Perchlorate (AP) salt due to its strong oxidizing property and has a decomposition profile similar to other common components of solid propellant, such as hydroxyl-terminated polybutadiene (HTPB) polymer. Despite its widespread use, and decades of research dedicated to the topic, there exists no consensus on the mechanism of its thermal decomposition or intermediate species within the crystalline salt. Ammonium Perchlorate is an ionic salt consisting of ammonium and perchlorate ions, forming solid NH_4ClO_4. There are two major theories existing on the mechanism of AP decomposition. The proton-transfer mechanism suggests that a hydrogen ion is transferred from the cation to the anion, forming ammonia and perchloric acid. The second theory on AP decomposition is the electron transfer mechanism, which proposes that the initial phase of decomposition happens when perchlorate ion donates an electron to the ammonium ion and both the components convert to the gaseous state.

1.1 Properties and Thermal Decomposition of Ammonium Perchlorate

Ammonium perchlorate is a white crystalline material, seen in Figure 1 that is orthorhombic at room temperature and undergoes a phase transition to cubic at 240°C. Thermal decomposition happens in two distinct stages: Low temperature decomposition (LTD) which happens between 300° and 380° and high temperature decomposition (HTD), which occurs above 380°. Figure 1 shows the transition between LTD and HTD. A clear inflection point exists in the weight loss profile of non-catalyzed AP decomposition. Low temperature decomposition nucleates at defect sites in the crystal lattice, and grows, creating a porous structure within the bulk of the crystal[3] The material experiences up to a 20% weight loss during this phase and the remaining crystalline material is chemically identical to the original material. It's believed the LTD phase is stunted by severe disorder in the crystal lattice, which becomes a major barrier to electron transfer within a crystal[4]. High temperature decomposition is characterized by sublimation of the remaining solid AP material leading to 100% weight loss of the initial material.

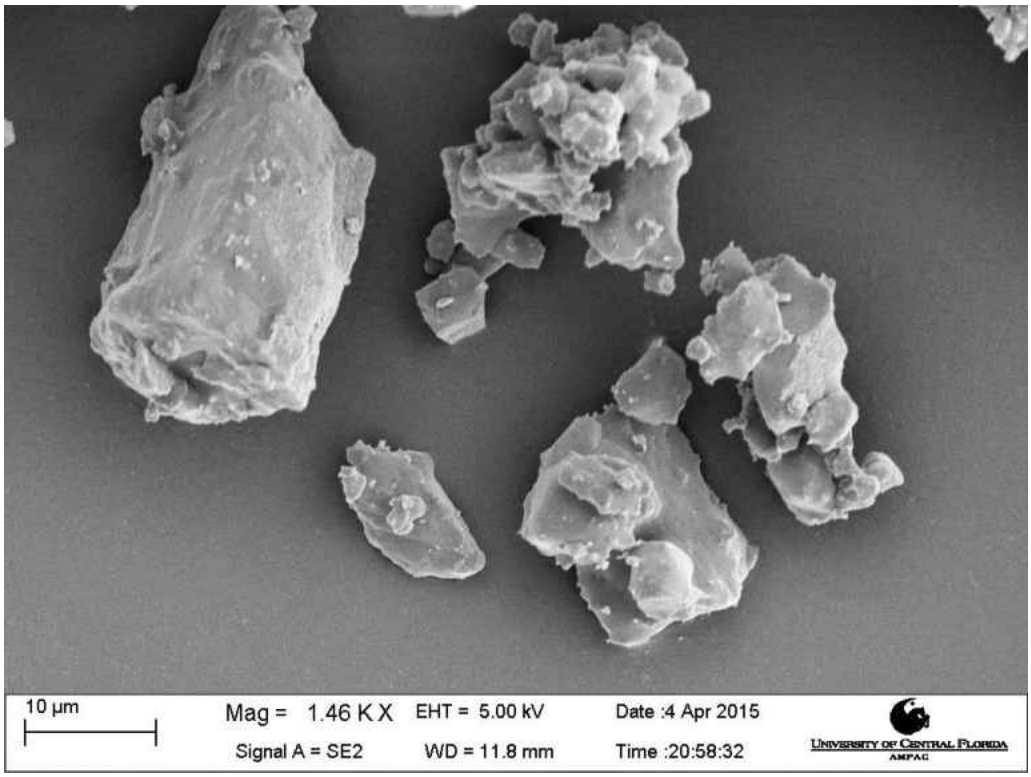

Figure 1: SEM image of AP crystals. Average size around 10 µm

The LTD produces more O_2 gas per mole of AP compared to the HTD. For this reason, it is advantageous to maximize the amount of decomposition occurring in the first phase when using AP as an oxidizer. The two major theories on the mechanism of AP decomposition are proton transfer mechanism and electron transfer mechanism which were first introduced by Jacobs in 1967[5] and Bircomshaw in 1955[3]

.

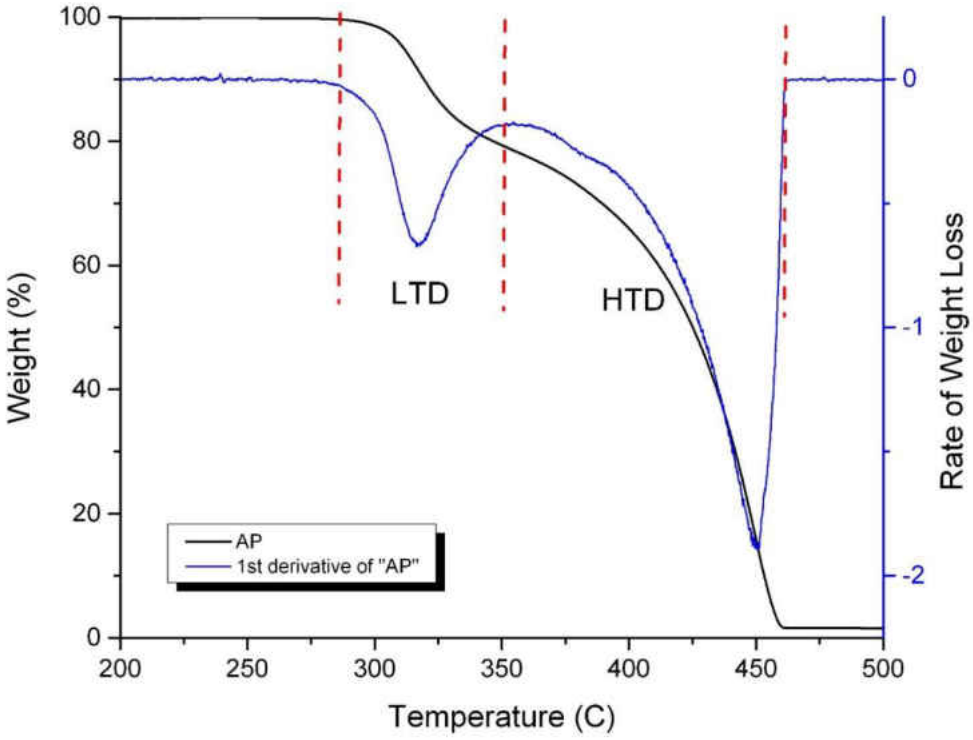

Figure 2: ThermoGravimetric decomposition profile of Ammonium Perchlorate. Two regions of rapid weight loss LTD and HTD.

The proton-transfer mechanism suggests that a hydrogen ion is transferred from the ammonium to the Perchlorate ion, forming ammonia and perchloric acid. The formed perchloric acid decomposes while the ammonia oxidizes and many sub-reactions occur after, which are summarized in figure 2. The second theory on AP decomposition is the electron transfer mechanism, which proposes that the initial phase of decomposition happens when the perchlorate ion donates an electron to the ammonium ion and both components convert to the gaseous state. After this, ammonium decomposes into ammonia and a hydrogen atom, which

reacts with the perchlorate ion to form perchloric acid, then goes on to decompose into water vapor and chlorine gas. These products then further react to form the final products of AP decomposition, which are mainly Cl_2, N_2O, O_2, H_2O. It is noted that the electron transfer is believed to be the rate limiting step in this process. A study by Heath, et al has also shown trace amounts of ClO_2, NOCl, NO_2 [3]. This process is summarized in Figure 3.

$$NH_4^+ + ClO_4^- \rightleftharpoons NH_3(a) + HCl_4(a)$$

$$HCl_4 \rightleftharpoons OH^- + ClO_3^-$$

$$2OH^- \rightleftharpoons H_2O(g) + \frac{1}{2}O_2(g)$$

$$2ClO_3^- \rightarrow Cl_2 + 3O_2$$

$$2NH_4ClO_4 \rightarrow 4H_2O + Cl_2 + O_2 + 2NO$$

Figure 3: The various sub-reactions occurring during thermal decomposition of ammonium perchlorate according to the proton transfer mechanism. [6]

$$ClO_4^- + NH_4^+ \rightarrow ClO_4^0 + NH_4^0$$

$$NH_4^0 \rightarrow NH_3 + H$$

$$HClO_4 + H \rightarrow H_2O + ClO_3$$

Figure 4:Summary of the electron transfer mechanism of AP decomposition.[7]

1.2 Catalysis of Ammonium Perchlorate Decomposition

In recent years, many studies have been done aimed at modifying the decomposition

profile of ammonium perchlorate. One way to achieve this is to introduce catalytic compounds to the AP. Catalytic effects on AP decomposition can manifest themselves in a number of different ways. A lowering of the decomposition temperature, an increase in the enthalpy of reaction, a decrease in the activation energy all show catalytic effects. Studies have been focused primarily on metals and metal oxides as a catalyst for decomposition. A review by Chaturvedi, et al summarizes the effects of adding nano metals into AP[8]. Cu, Ni and Al nanoparticles were compared by their catalytic effects. It was seen that the Cu lowered the temperature of the exothermic peak by 35.1°C, while Ni and Al increased the exothermic temperature by 3.9°C and 5.9°C respectively. It was also seen that the heat output of the reaction was increased by using Ni, Cu and Al additives by 1.32, 1.20 and 0.903 kJ/g respectively. Duan, et al showed similar results by looking at high loadings of Ni powder in AP. It was shown that a 25 wt% Ni in AP mixture lowered the decomposition temperature by 100°C and increased the heat output by almost 800 J/g compared to pure AP[9], which is in disagreement with the findings of Chaturvedi. Hermony and Salmon performed a study comparing different additive's catalytic activity in the very low temperature range of 170°-200°C, well before the AP crystals undergo the characteristic phase transition at 240°. The results of their study are shown in Figure 4, which shows the percent decomposition, α, of several catalyzed AP mixtures as a function of time at constant temperature[10]. Metal oxides are also shown to lower the activation energy of the decomposition of AP by a considerable amount[11]. Another study also showed that transition metal fluorides had a catalytic effect on the decomposition of AP[12]. However this effect was considerably small than that of their oxide counterparts.

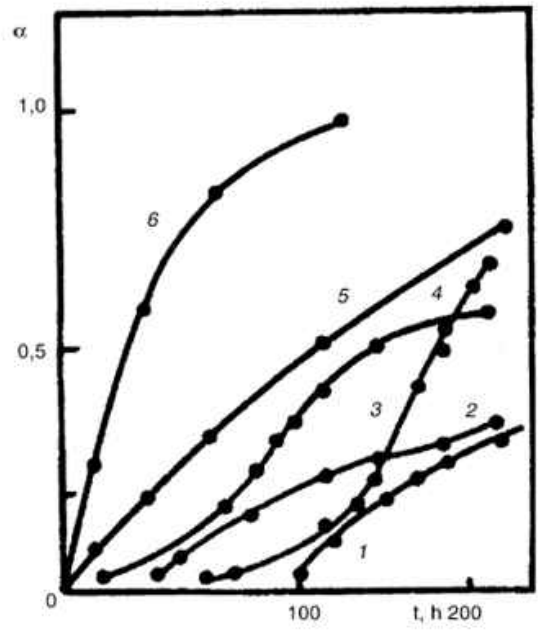

Figure 5: Catalytic activity of various additives on the thermal decomposition of AP at temperature less than 200°C. (1)AP; (2) AP + MgO; (3)AP +Cr_2O_3, (4)AP+MnO_2 (5)AP+(Co_2O_3+Co_3O_4)[7]

A study by Chatirvedi, et al showed that nano-alloys can catalyze the HTD of AP and lower the activation energy by as much as 71%[8] A study by Galway suggests that the presence of nitrates in AP salt has a drastic effect on the decomposition behavior. They proposed that nitryl pechlorate exists as an unstable intermediary in the decomposition. The ionic bond between perchlorate and ammonia ions is substituted by the covalent bond between the nitrate species and perchlorate, forming NO_2ClO_4, which is very unstable at reaction temperature, and will therefore quickly dissociate and allow the nitrate species to further decompose the AP salt. A mixture of ammonium nitrate mixed with AP was isothermally heated and measured for degree of decomposition over

time as shown in Figure 5. 5wt% of the nitrate species has a drastic impact on the decomposition rate of AP salt[13]. Further studies on the effect of nitrates on AP decomposition have not been done.

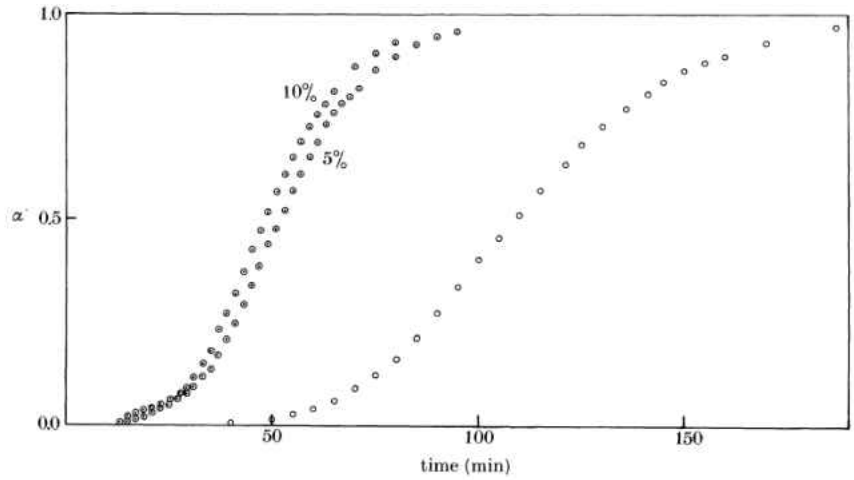

Figure 6: Comparative fractional reaction α-time plots for the decomposition at 503K of AP crushed powder and mixtures of AP with 5 and 10% ammonium nitrate.

1.3 Boron Nitride Nanostructures

Boron Nitride (BN) is a material made of equal amounts Boron and Nitrogen. The recent rise in interest in Boron Nitride is a result of the enormous study on graphene as BN can form identical structures with very similar properties. BN is an attractive material for many applications due to its high thermal and chemical stability. BN comes in 4 main phases; cubic, rhombohedral, hexagonal and wurtzite, depicted in figure 6. The two most common structures are cubic, which tends to be more densely packed and resembling bulk material and hexagonal, which is more common when synthesizing nanomaterials. The transition temperature between cubic and hexagonal BN has long been debated and is very sensitive to

defects, purity and grain size[14]

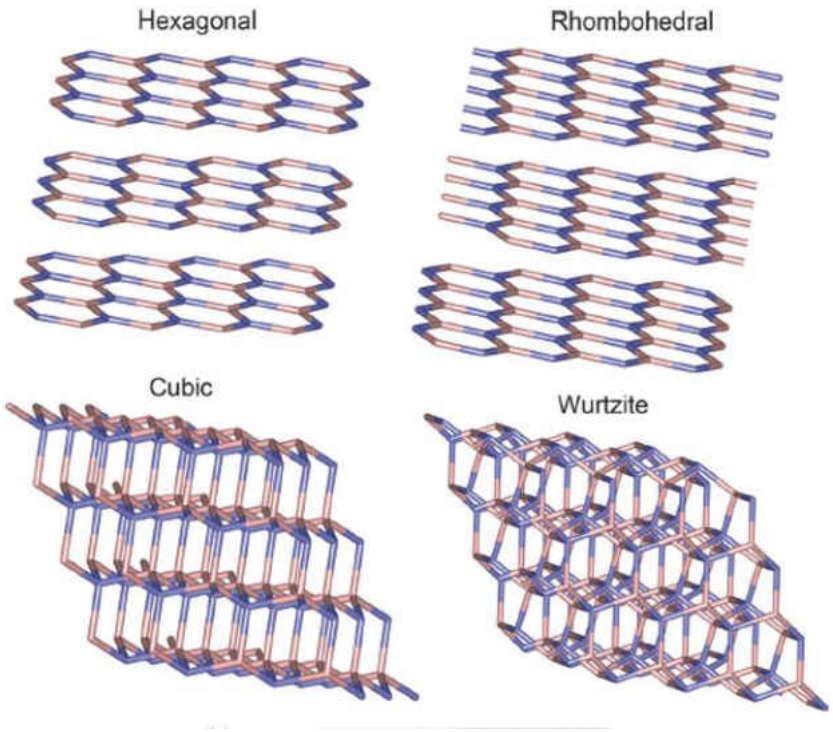

Figure 7: Illustration of structure of the four main phases of boron nitride. Cubic and hexagonal are the most widely studied[15]

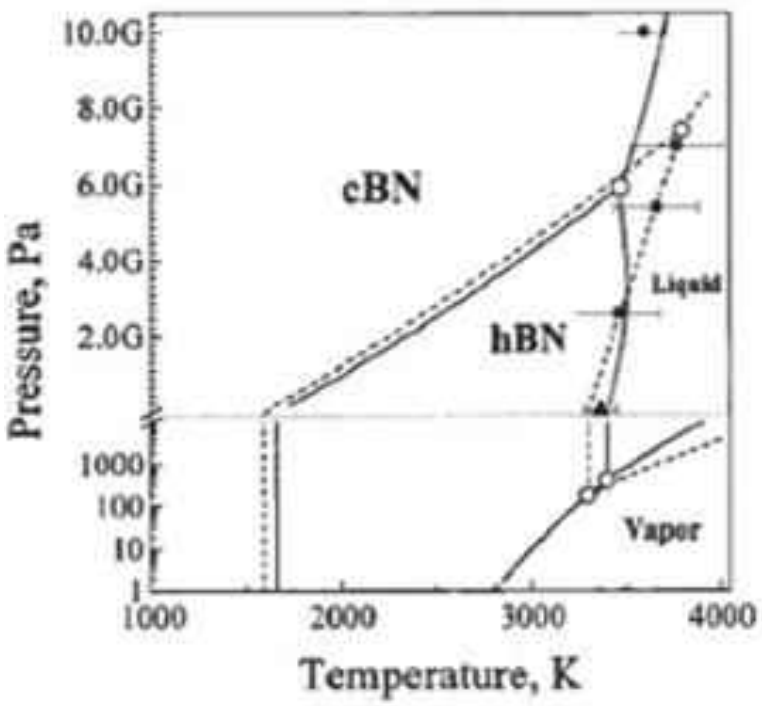

Figure 8: Phase diagram of Boron Nitride[15]

The most common form of defect found in hexagonal BN is a Stone-Wales defect, in which the hexagonal ring connecting 6 atoms becomes a pentagonal ring connecting 5 atoms. This type of defect is also very commonly found in graphene. These defect sites are more chemically active and are more prone to functionalization compared to pristine defect-free boron nitride sheets[16]. The wide band gap (5-6ev), chemical stability and thermal conductivity of BN has given it applications in a variety of areas. BN has been used as a substrate for graphene devices in electronics[17], as thermal fillers in polymers[18], as wettability modifiers[19] and has been shown to increase the fracture toughness of composite material at loadings of 1wt% by as much as 22%[20]. However, no studies have shown BN being directly used as a catalyst in thermal decomposition reactions.

1.4 Decomposition of AP using BN

It was recently discovered that a small amount of boron nitride mixed with ammonium perchlorate has a drastic impact on the burn characteristics of the AP powder.

Boron nitride material can be advantageous for use in propellants compared to the more commonly used iron oxide because it has a much lower molar weight, has a facile synthesis process, is relatively inexpensive and creates a preferable decomposition profile of AP compared to the more commonly used iron oxide nanopowder.

The purpose of this study is to determine if BN can be competitive with iron oxide as an AP decomposition catalyst and if the BN acts as a true catalyst or if the material undergoes chemical changes thoughout the process.

CHAPTER TWO: METHODOLOGY

Four variations of boron nitride material were synthesized in a hydrothermal reactor and fully characterized by X-Ray Diffraction (XRD), Scanning Electron Microscopy (SEM), Transmission Electron Microscopy (TEM), X-Ray Photoelectron Spectroscopy (XPS) and Brunauer–Emmett–Teller (BET) analysis. The material was then mixed with ammonium perchlorate salts and ground together to form a uniform dispersion. DSC studies were done to measure the catalytic effect of the BN on the AP decomposition. SEM images were taken of the AP crystals at various degrees of decomposition. FTIR spectra were recorded of the BN material before and after participating in the decomposition of AP. Other experiments were performed to illustrate the catalytic nature of the BN when mixed with AP.

2.1 Boron Nitride Synthesis

The boron nitride was synthesized via a hydrothermal method as described by Li, et al[21]. H_3BO_3 was mixed with $C_3N_6H_6$ and a small amount of 0.1M HNO_3 was introduced to adjust to pH to 6.5. Then a triblock copolymer was added as a template. The mixture was stirred vigorously and heated to 85°C for 6 hours and then cooled to room temperature. A white precipitate formed and the mixture was filtered and dried in a vacuum oven to remove any residual water. The literature procedure calls for activation of BN by heating at 1300°C for 8h but this step was forgone for our synthesis. The material was varied by adding different amounts of each precursor in an attempt to synthesis non-stoichiometric BN materials and no template polymer was used in the synthesis of the BN-4 sample. Table 1 summarizes the amount of each precursor and template

used for the synthesis of each BN sample.

Table 1: Concentrations of reagents used in BN synthesis.

Sample	H_3BO_3 (Boric Acid)	$C_3N_6H_6$ (Melamine)	Template
BN-1	3.71g, (0.3 M)	3.78g, (0.15 M)	P123
BN-2	5.71g, (0.46 M)	1.78g, (0.07 M)	P123
BN-3	1.71g, (0.14 M)	5.78g, (0.23 M)	P123
BN-4	3.71g, (0.3 M)	3.78g, (0.15 M)	No Template

2.2 Differential Scanning Calorimetry/ Thermo-Gravimetric Analysis Measurements

Differential Scanning Calorimetry (DSC) was performed on samples of 5 wt% BN in AP for all four varieties of BN as well as 5 wt% Fe_2O_3 in AP, 5 wt% TiO_2 in AP, 5 wt% silver nitrate and 5 wt% cerium (III) nitrate hexahydrate and pure AP under argon up to a temperature of 500°C at a heating rate of 30C/min and as well as 20C/min and 10C/min Sample size varied between 5-6mg. This data was used to calculate the activation energy of LTD of AP for each sample. The heat output, decomposition temperature and LTD weight loss was also calculated from the DSC/TGA plot. A TA Instruments SDT Q600 was used to perform these measurements.

2.3 X-Ray Diffraction

The X-ray diffraction patterns were collected using Rigaku D/MAX XRD with CuKα source (λ=0.1541 nm) at a scan rate of 0.01°/step over 20-70° (2θ) range.

2.4 Fourier Transform Infrared Spectroscopy

FTIR Spectroscopy is a technique that allows the examination of chemical composition of a solid sample based on the natural vibrational frequencies of the interatomic bonding in the matierl. A Perkin Elmer Spectrum One FT-IR Spectrometer was used in conjunction with athe ATR accessory. For this experiment, the BN samples were placed in an oven at 600°C. 5 wt% BN samples in AP were also put in an oven at 600°C to fully decompose the AP, leaving just the BN catalyst as a residue. FTIR spectra were taken of each sample (pure BN and the residue from AP decomposition). 12 scans were done per spectrum from 4000 to 650 cm^{-1} at an interval of 4 cm^{-1}. The purpose of this experiment is to determine the difference in chemical composition between the heated BN and the BN that has catalyzed AP decomposition.

2.5 Scanning Electron Microscopy Studies

SEM images were taken of partially decomposed AP crystals using a Zeiss ULTRA-55 FEG SEM. The samples were partially decomposed AP crystals, 5 wt% BN in AP samples were heated by the DSC up to a specific temperature, which correlated to a specific degree of decomposition, and then the reaction was quenched by opening the DSC furnace and removing the crucible that contained the material. This process was done 3 times for each variety of BN, Once at minimal

decomposition of AP, once at the midpoint of LTD and once for the complete LTD of AP. SEM was also used to image the pure BN samples as well as the residue left from the completed reaction of BN/AP samples. Characterization of the pure BN material is also done to be compared to that of the material after participating the decomposition reaction.

CHAPTER THREE: RESULTS AND DISCUSSION

It's expected that the boron nitride material participates in the decomposition reaction. The material, even in small amounts is expected to be consumed, or partially consumed by the AP decomposition reaction. It's likely that intermediate products of the decomposition including nitrogen species' will be in a greater concentration during the reaction's that include catalyst material as can be shown by the FTIR.

3.1 Boron Nitride Nanopowder Characterization

Full characterization was done on all four BN samples including XPS, SEM, TEM, XRD, BET. SEM was done to boron nitride samples as well as AP/BN mixtures to see the morphology of the samples and how the pore size during decomposition is effected by the presence of the catalyst material. XPS was used to determine the relative composition of the material before and after participation in the decomposition reaction. TEM will be used to determine structure, relative composition and crystallinity. BET will be used to determine suface area and pore size of the boron nitride material.

3.1.1 SEM images of Boron Nitride and AP decomposition

Figure G shows SEM images of all four variations of BN. BN-1, BN-2, and BN-4 all formed ribbons. BN-1 ribbons are roughly 0.5 micron wide and approximately 10-15 micron long. BN-2 ribbons are 10 microns wide and between 300 to 400 microns long. BN-4 ribbons are 2 microns wide and between 30 and 50 microns wide. BN-3 formed irregularly shaped, stone-like

structures that are about 100 to 200 microns in size. It is noted that the materials which have an ample amount of boron present were able to form ribbons while the boron deficient material was unable to form a structure which existed as a nanostructure in any dimension. The boron-deficient material formed a bulk structure resembling pebbles, which suggests that having sufficient Boron in the material is crucial for keeping the ribbon-like amorphous structure seen in all 3 other samples.

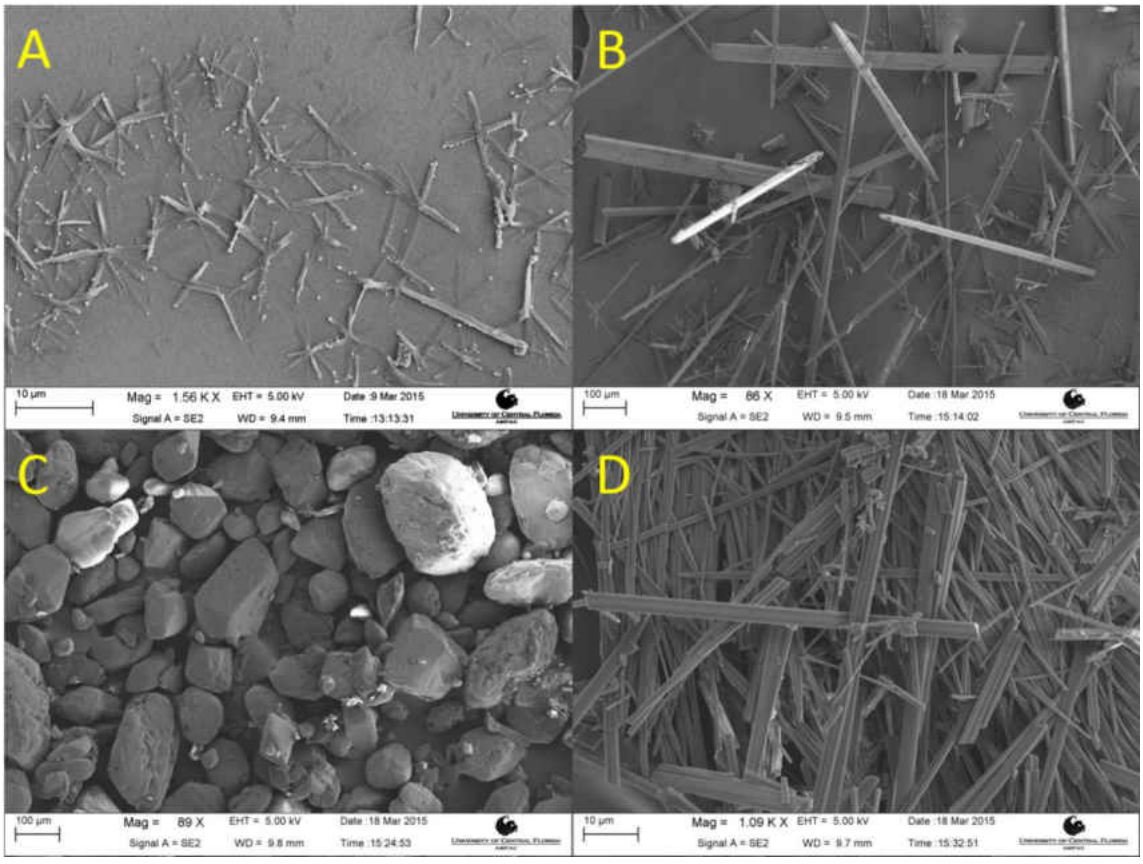

Figure 9: SEM images of hydrothermally synthesized Boron Nitride samples. A)BN-1 B)BN-2 (boron rich) C) BN-3 (nitrogen rich) D) BN-4 (high surface area)

To study the nature of AP decomposition, it is advantageous to see the surface morphology of the AP at various stages of decomposition. To achieve this, samples of AP mixed with 5wt% of BN material which were heated in the DSC cup to 330°C and 360°C which correspond to the early stages of LTD and the end of LTD, respectively. Immediately after heating, the sample was quickly removed from the heat and the decomposition reaction was quenched. SEM images were taken of the AP/catalyst samples to show the morphology of thermal decomposition. Figure 9 shows SEM images of pure AP after being decomposed without the use of a catalyst. The pores on the surface of the crystal are from the decomposition and is the mechanism by which the material experiences weight loss during thermal decomposition.

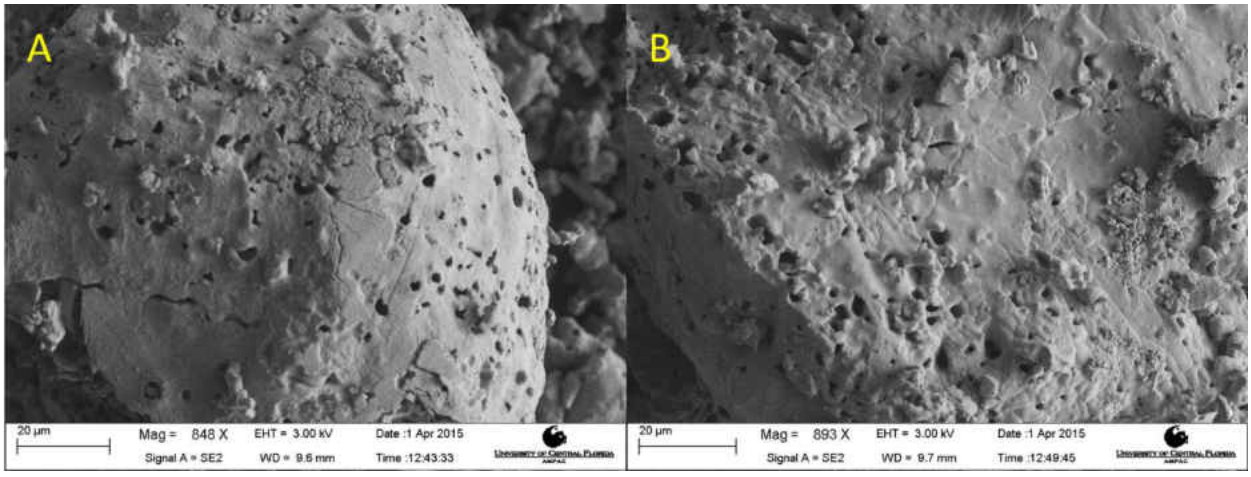

Figure 10: SEM images of uncatalyzed AP crystals heated to A) 330°C and B) 360°C pore size increases as the degree of decomposition increases.

Figure 8 shows the SEM images of AP crystals heated to 330°C and 360°C when in the presence of BN-1. Very small changes on the surface of the AP crystal occur when heated from 330° to 360°C. The TGA data shows the pure AP sample heated to a temperature of 330°C experienced a 5.8% weight loss and the sample heated to 360°C experienced a 14.2% weight loss.

Figure 9 shows the SEM images of the AP crystals heated to 330°C and 360°C when in the presence of BN-2. The samples heated to 330°C and 360°C experienced weight loss of 13.2% and 77.8% respectively. Similar to the decomposition of AP with BN-1, the AP with BN-2 mixture created more and larger pores on the surface of the AP crystal causing a much higher degree of decomposition of the AP crystals which allowed the AP to lose more than double the weight during LTD compared to the uncatalyzed AP crystals.

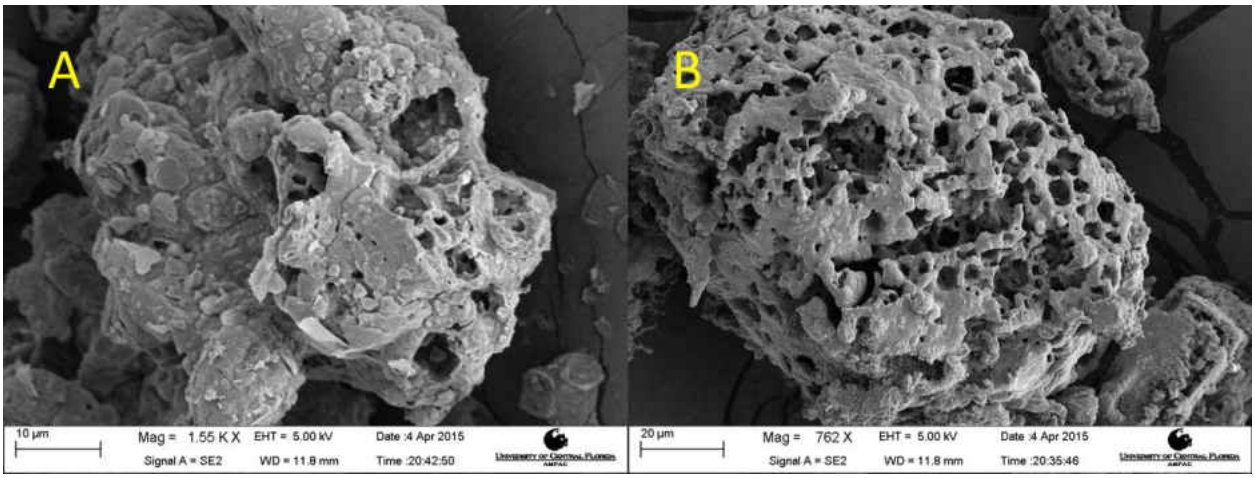

Figure 11: SEM images of AP crystals after being heated to A)330°C and B)360°C, Both heated in the presence of BN-1

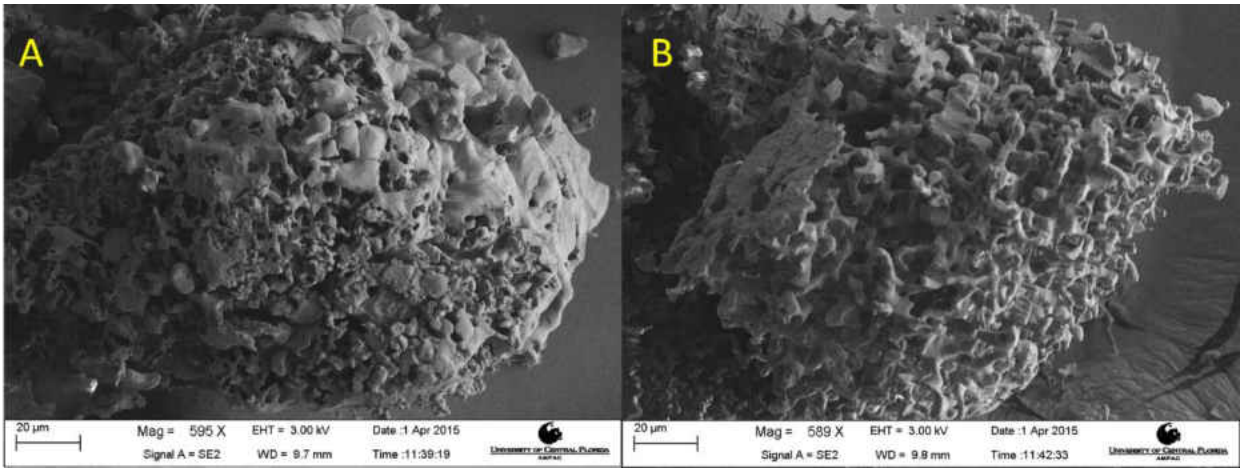

Figure 12: SEM images of AP in the presence of BN-2 after heated to A)330°C and B)360°C. The catalyst material produces a fast increase in the degree of decomposition.

Figure 10 shows the SEM images of the AP crystals heated to 330°C and 360°C when in the presence of BN-3, which went through a weight loss of 2.0% and 41.6% respectively. The AP/BN-3 mixture also caused a much higher deformation of the surface of the AP crystals which allowed the AP to lose more than double the weight during LTD compared to the uncatalyzed AP crystals.

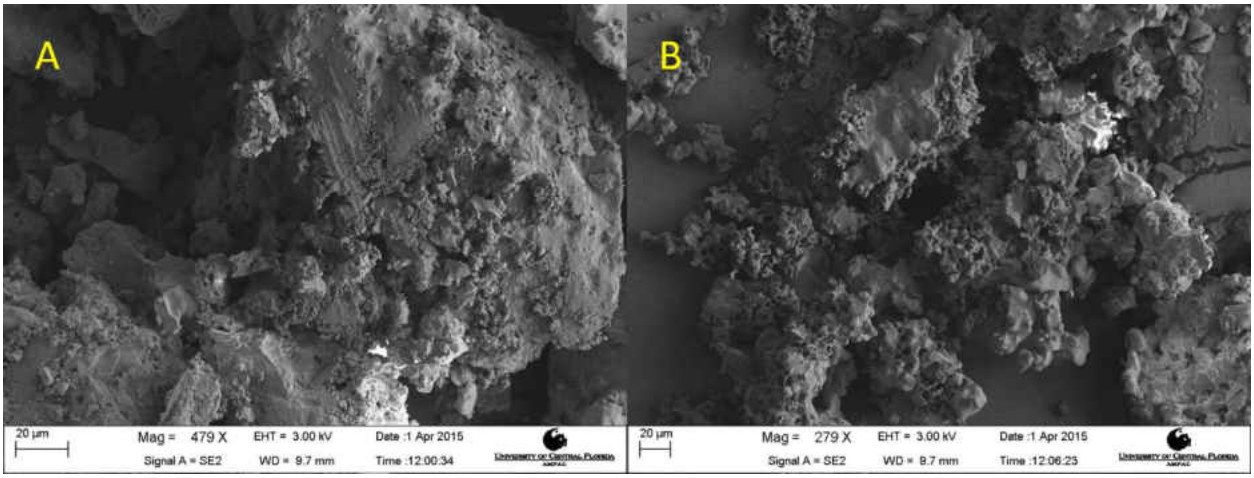

Figure 13: SEM images of AP after heated to A)330°C and B)360°C in the presence of BN-3. The catalyst material produces a drastic amount of decomposition in the range of 330°C to 360°C.

Similar results are obtained from AP decomposition in the presence of BN-4. Figure 12 shows the SEM images. The samples heated to 330° and 360°C lost 3.9% and 54.6% of their original weight, respectively.

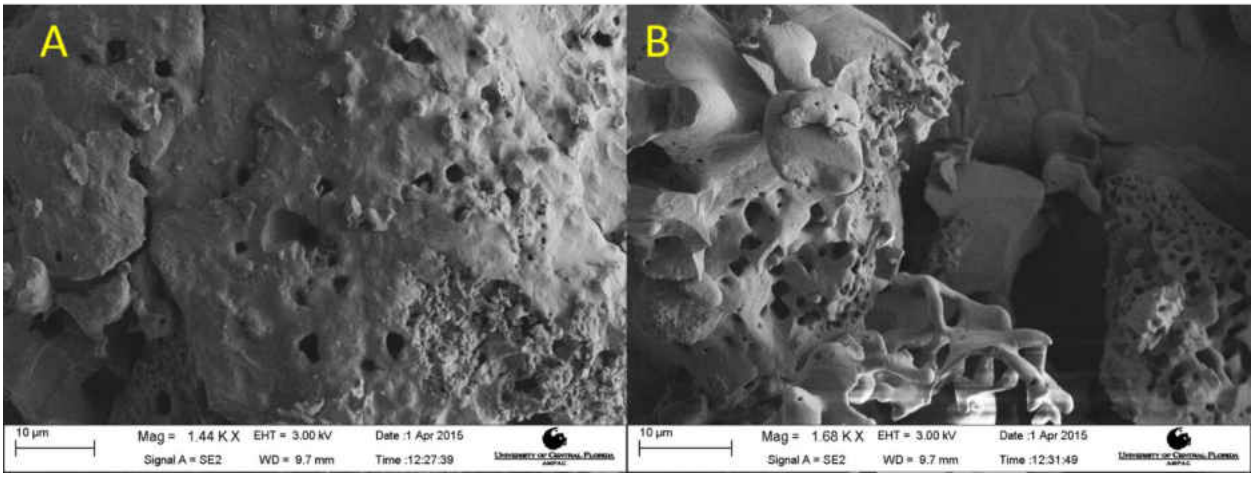

Figure 14: SEM images of AP after heated to A)330°C and B)360°C in the presence of BN-4

The SEM study on the degree of decomposition at varying temperatures shows that the BN material is having a large impact on the nucleation and growth of the pores in the AP crystals, through the gases formed as a result of AP decomposition are escaping faster, causing a large weight loss in the material.

SEM images were also taken of the residue of the catalyzed AP decomposition. The AP is known to completely decompose when uncatalyzed so the residue of burning the AP is assumed to be completely the BN catalyst material. Figure 13 shows SEM images of post-decomposition catalyst material. The catalyst material clearly goes through a complete topological change. BN-1, BN-2, and BN-4 samples no longer resemble nanoribbons and BN-3 might show some amount of resemblance to the rock-like structure it shows prior to burning, but shows a very porous version.

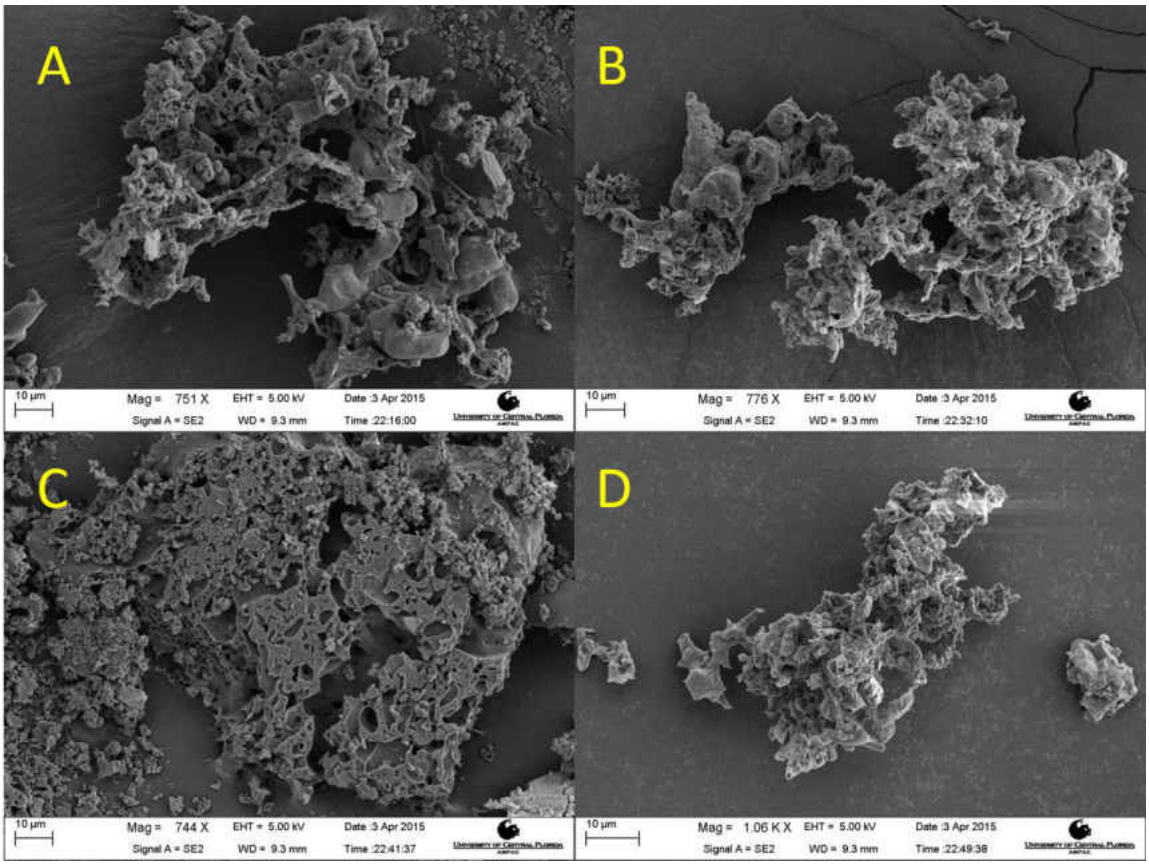

Figure 15: SEM images of catalyst material after complete decomposition of AP. A)BN-1 B)BN-2, C)BN-3, D)BN-4

3.1.2 TEM

Figure 14 shows TEM image of a ribbon from BN-1. A white circle is superimposed on the image to display the selected area used to take the SAED pattern shown in figure 15. Figure 16 shows the EELS spectra from the same area with the boron, carbon, nitrogen and oxygen peaks labeled. The SAED pattern confirms a lack of crystallinity in the material and the EELS spectra confirms the presence of Boron, Carbon, Nitrogen and Oxygen, which is consistent with the

findings of Li, et al[21]

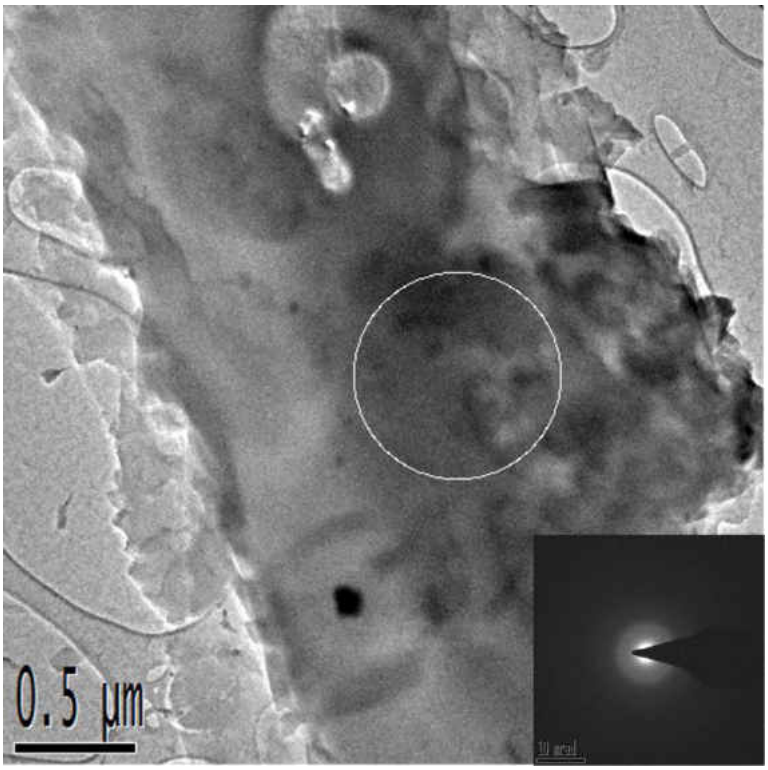

Figure 16: TEM image of BN-1 sample and corresponding SAED pattern. White circle represents location of Selected Area Aperture

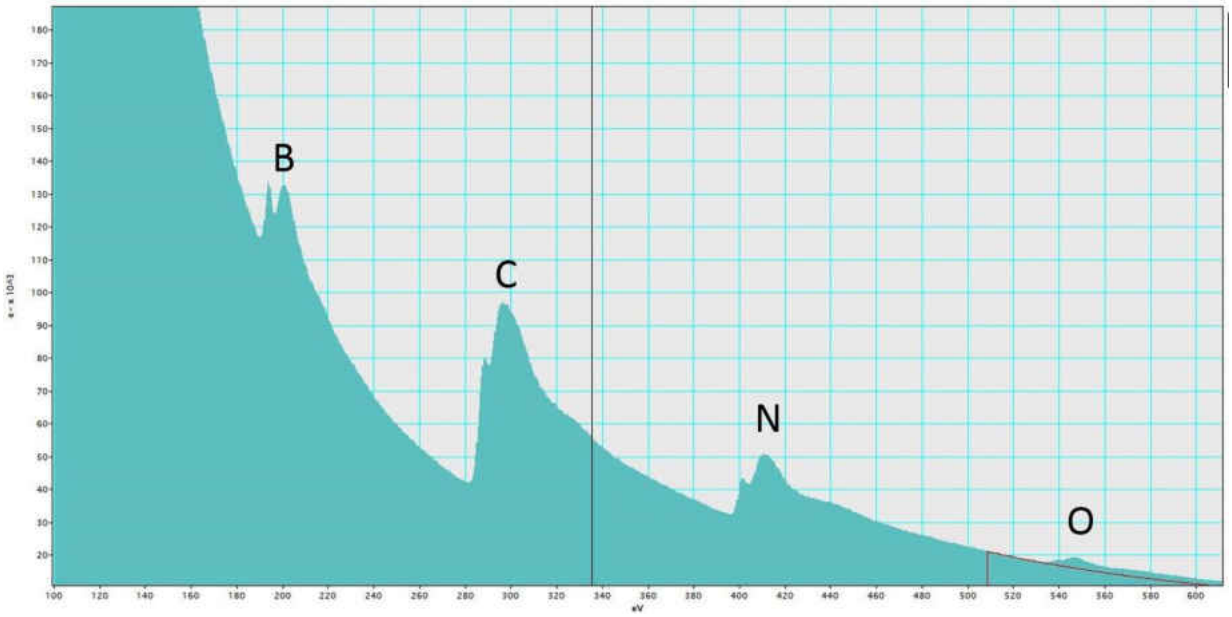

Figure 17: EELS spectra of BN-1. Boron, carbon, nitrogen and oxygen are all present in our BN material.

3.1.3 BET

The BET showed the surface area of BN-1, BN-2, BN-3, and BN-4 to be 22.708, 22.53, 7.875 and 41.069 $\frac{m^2}{g}$, respectively. The considerably low surface area of BN-3 is due to the large particle size produced compared to the other BN samples.

3.1.4 Differential Scanning Calorimetry/ Thermo-gravimetric analysis

DSC/TGA was done on samples of 5wt% catalyst material in AP. The catalysts examined were the four BN variations as well as nano-scale Fe_2O_3, boron powder, as well as silver nitrate, and cerium nitrate, which were chosen to compare to the BN material in the case that the BN may

have nitrate species in the material. Figure 17 shows the weight loss profiles for Pure AP, BN-1, BN-2, BN-3, BN-4 as well iron oxide. The graph clearly shows a very rapid weight loss for the material containing catalysts as well as an expansion of the total weight loss from LTD.

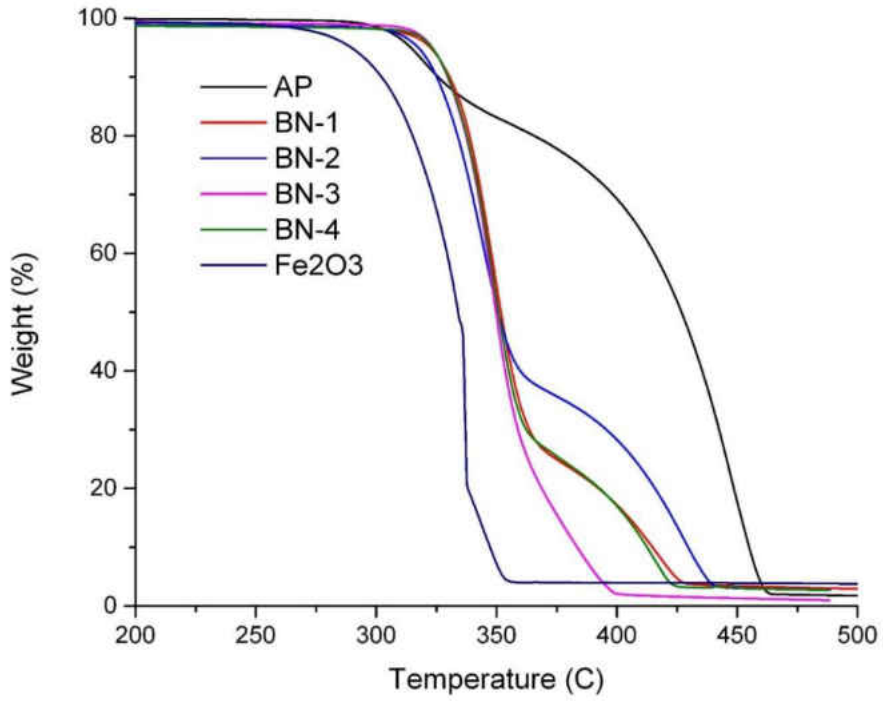

Figure 18: TGA graph of thermal decomposition of AP in which 5wt% of various catalysts are mixed. A trend is shown between the decomposition characteristics and the concentration of nitrogen

From the TGA plot we can see a trend in the activity of the BN catalysts based on the composition. Through the early stages of LTD, in all cases the AP/BN mixtures follow the same profile. The samples with higher amounts of nitrogen present, such as BN-3, produce a larger weight loss before entering HTD. BN-2, which has the lowest amount of nitrogen present produces a weight

loss of 60.77%, BN-1 and BN-4, which have equal amounts of nitrogen produce a weight loss of 72.23% and 70.64%, respectively and BN-3, which has the highest amount of Nitrogen produces a weight loss of 77.21%. This suggests the magnitude of decomposition during the LTD is directly linked to the presence of nitrogen. Figure 17 shows the first derivate of the weight profile with respect to temperature. It's shown that the mixture with BN-3 in it has the highest instantaneous weight loss during the LTD, then BN-2 and BN-3 have similar rates of weight loss, followed by BN-2 which has the lowest rate of weight loss, following the similar trend related to the amount of nitrogen in the sample. The rapid weight loss of BN-3 is very desirable for applications in propulsion because to get a large impulse on a ship, you need to apply a very large force in a short amount of time. This is achieved by the rapid weight loss seen from the AP mixture with BN catalyst. Figure 18 shows the rate of weight loss for the AP and BN-3 mixture compared to the mixture of AP and Fe2O3. The BN-3 mixture has a higher rate of weight loss during its LTD compared to the LTD of Fe2O3, but the Fe2O3 material experiences a very rapid weight loss of the remaining 20% of material during HTD, giving it a very large spike in rate of weight loss.There is also a similar trend from the DSC heat flow data, which is shown in figure 20. We see from the DSC data that the catalysts produce a large exothermic peak compared to the pure AP decomposition plot. Again, we see a trend of the catalytic activity of the BN materials based on the Nitrogen content. BN-3 has the highest exothermic peak, followed by BN-1 and BN-4, which have relatively similarly sized peaks. BN-2, the lowest nitrogen content sample, has the smallest exothermic peak. The exothermic peak for BN-3 is comparable in size to that of Fe_2O_3, which itself shows a downward shift in peak position by about 20 degrees Celsius. The peaks positions for the BN/AP mixtures were all relatively the same, but showed a small downward

shift from the more catalytic sample to the least catalytic sample. The heat output was examined in the DSC software by integrating the area under the exothermic peak corresponding to the LTD for each sample. The pure AP sample has a heat output of 286.8$\frac{J}{g}$, the Fe_2O_3 sample has a heat output of 1412 $\frac{J}{g}$, and BN-1,2,3,4 have values of 1184, 912, 1352 and 1132 $\frac{J}{g}$ respectively. The onset temperature for the AP decomposition also changes depending on the catalyst material present. The onset temperature is calculated in the DSC/TGA analysis software. For pure AP, the onset temperature is 303.4°C, and for Fe_2 the onset temperature is 285.9°C, almost 18°C lower than the pure AP. The onset temperatures for BN-1,2,3,4 are 326.6, 318.4, 323.4, and 323.4°C respectively, which represents an increase of 23.2, 15.0, 20 and 19.8°C respectively. Samples with BN material show an upward shift in onset temperature while the Fe_2O_3 sample shows a downward shift in onset temperature compared to the pure AP. The heat output, decomposition onset temperature and LTD weight loss data are summarized in table 2.

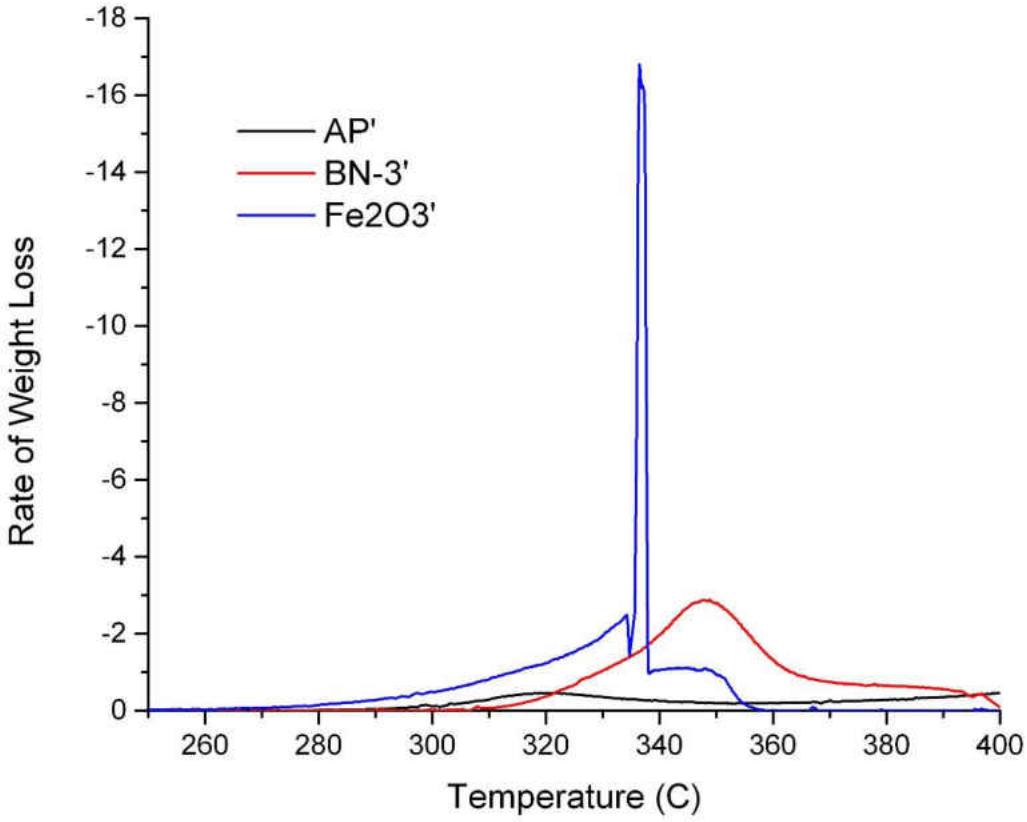

Figure 19: Rate of weight loss for AP mixed with 5w% catalyst materials.

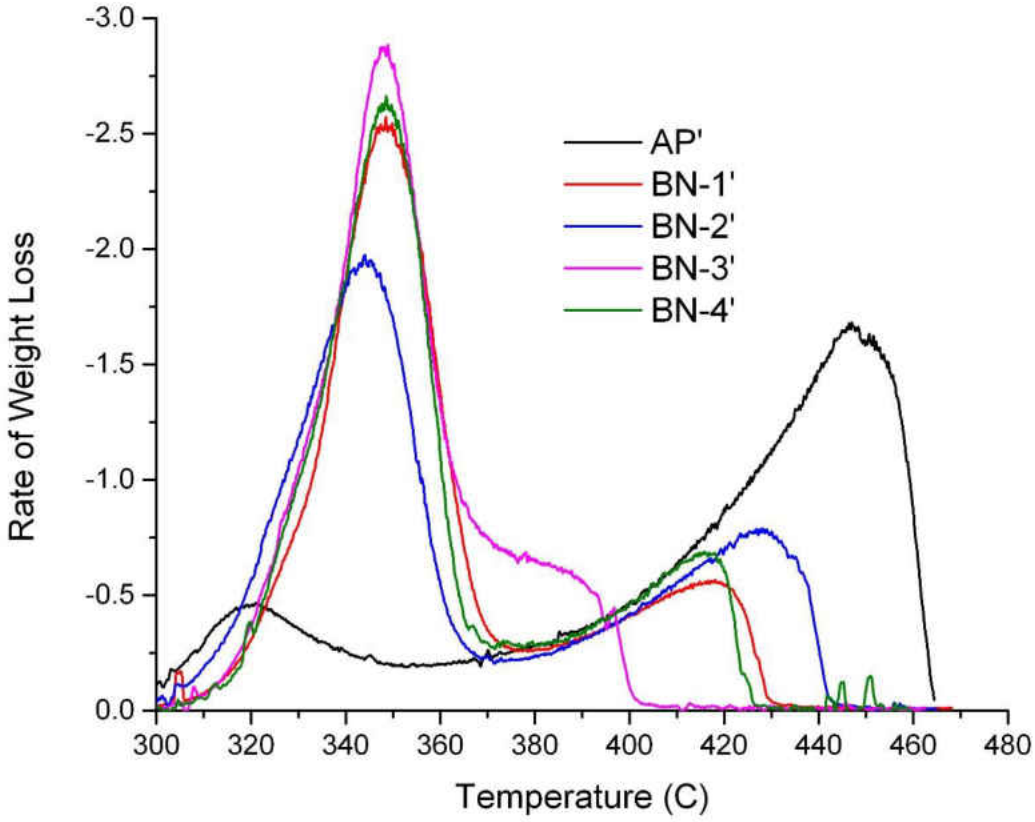

Figure 20: Rate of weight loss for AP mixed with 5wt% catalyst material. BN-3 shows the highest rate of weight loss during LTD.

Table 2: Summary of Heat Flow and Weight Loss Data from LTD of AP mixed with various catalyst material. BN and Iron Oxide catalysts increase the heat output of AP salt

Sample	Weight Loss During LTD (%)	Heat Output (J/g)	Decomposition Onset Temperature (Celsius)
Pure AP	13.84	286.8	303.41
BN-1	72.23	1184	326.6
BN-2	60.77	912	318.4
BN-3	77.21	1352	323.4
BN-4	70.64	1132	323.2
Fe_2O_3	80.52	1412	285.91

The activation energies of these mixtures were calculated using the Kissinger method[22]. By heating the material at two different heating rates and measuring the position of the exothermic peaks for each trial, the activation energy can be calculated using the following equation.

$$E = -R\frac{ln\left(\frac{\beta_1}{\beta_2}x\left(\frac{T_{\max 2}}{T_{\max 1}}\right)^2\right)}{\left(\frac{1}{T_{\max 2}}-\frac{1}{T_{\max 1}}\right)}$$

Where β is the heating rate, T_{max} is the position of the exothermic peak, R is the gas constant and E is the activation energy. Table 3 shows the heating rates, temperature and activation energies

of decomposition of AP and AP mixed with 1wt% BN catalyst materials.

Table 3: Summary of activation energy measurements and calculation of 1 wt% BN samples in AP

Sample	Heating rate (K/min)	Exotherm Peak (Celsius)	Activation Energy (kJ/mol)
Pure AP	30	337.27	97.3
	20	325.8	
1 wt% BN-1 in AP	30	348.27	84.1
	5	292.56	
1 wt% BN-2 in AP	30	356.4	90.7
	10	322.49	
1 wt% BN-3 in AP	30	363.4	99.8
	20	351.26	
1 wt% BN-4 in AP	30	349.9	103.5
	10	320.2	

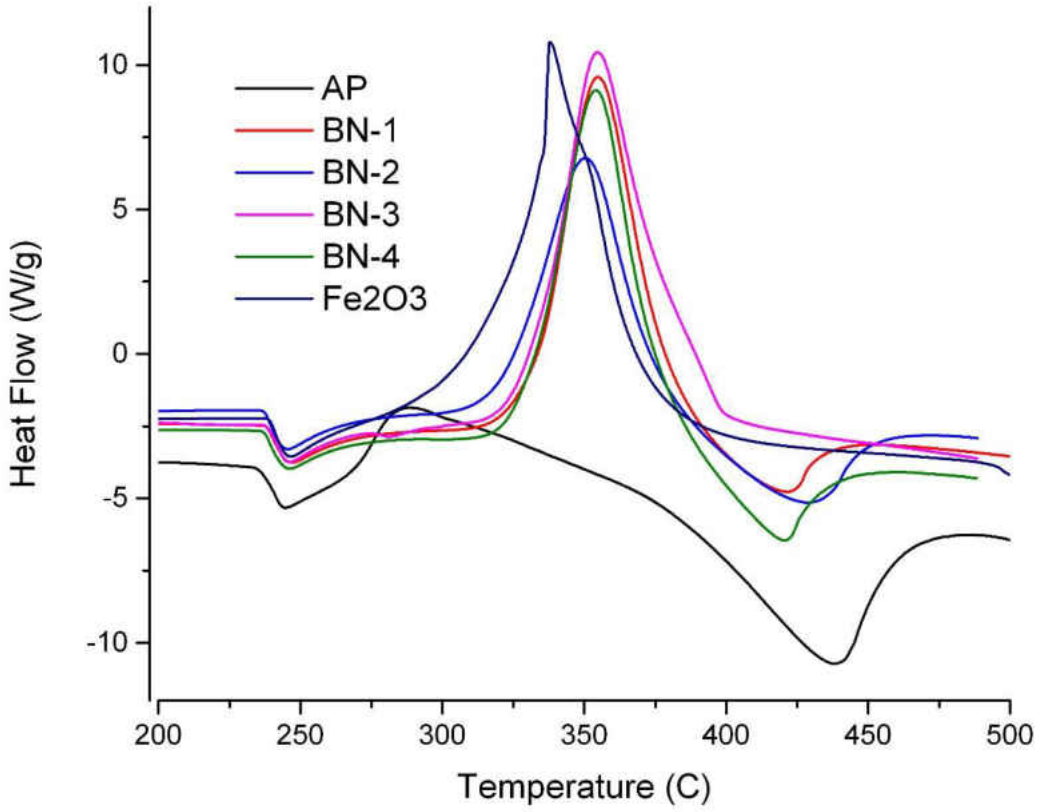

Figure 21: DSC plots of AP decomposition mixed with 5wt% catalyst materials. A trend exists between the nitrogen content in the catalyst material and the decomposition profile.

3.2 Compositional Analysis

Compositional analysis was done on the catalyst material to ensure that boron nitride is the main component of the powder.

3.2.1 X-Ray Diffraction Analysis

X-ray Diffraction was done on all BN samples. XRD patterns are shown in Figure 22

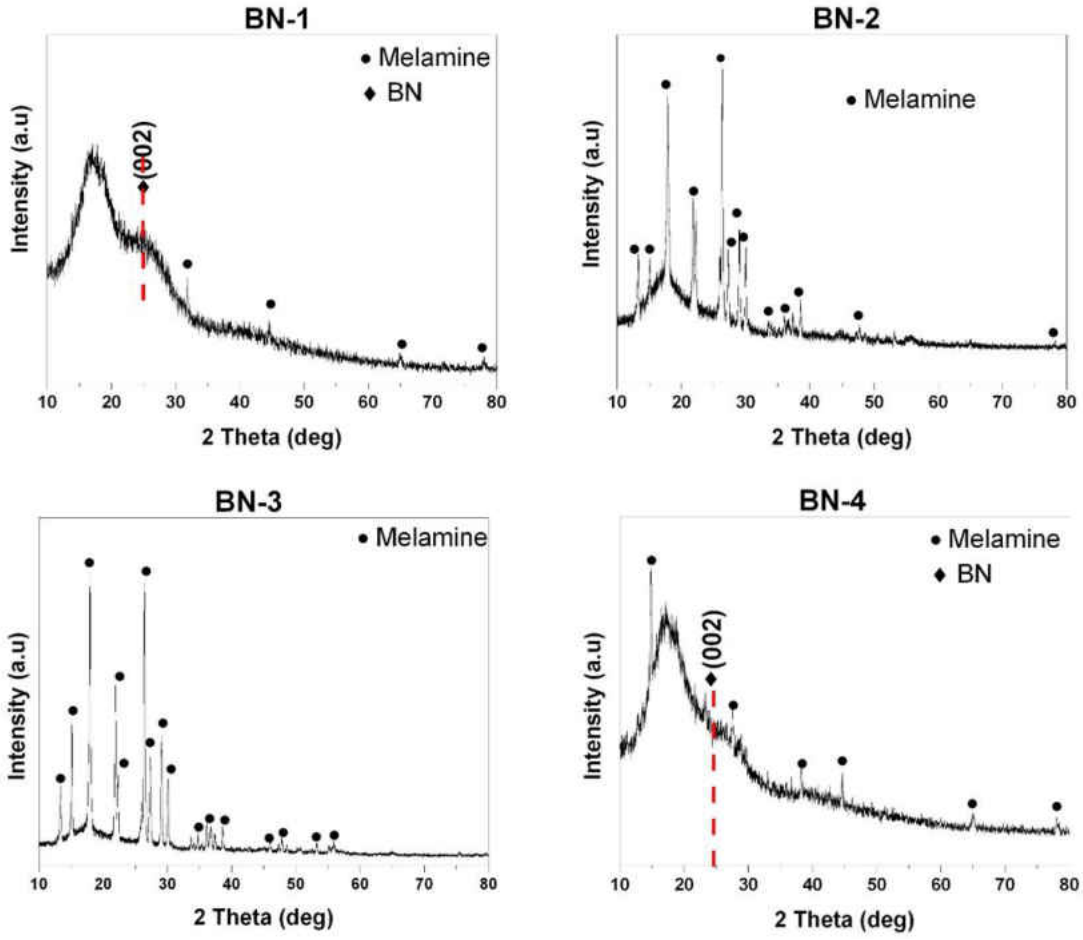

Figure 22: XRD of BN samples showing no crystallinity in BN-1 and BN-4 and crystallinity in BN-2 and BN-3.

All samples showed an amorphous hump from the BN as well as distinct peaks belonging to melamine, one of the precursors used in the synthesis. This suggests that there is residual precursor in our BN material that was not removed during the filtering process.

3.2.2 Fourier Transform Infrared Spectroscopy Analysis

FTIR was done on two sets of samples. The first set was the pure catalyst material heated to 600°C. The second set was 5wt% BN material in AP heated to 600°C. This was done to compare the chemical composition between the catalyst material when in the presence of AP during heating and not. A difference in chemical composition between the two sets of samples would suggest that the BN material goes through a different reaction when in the presence of AP and therefore plays a chemical role in the AP decomposition and undergoes a permanent chemical change. Figure 23 shows the FTIR spectra of these two sets of data (samples heated in the presence of AP labeled BN-X in AP).There exists a very clear difference in composition between the catalyst before and after the decomposition. In most cases, the characteristic peaks change when in the presence of AP. Although for the case of BN-3, the spectrum with and without AP is essentially unchanged.

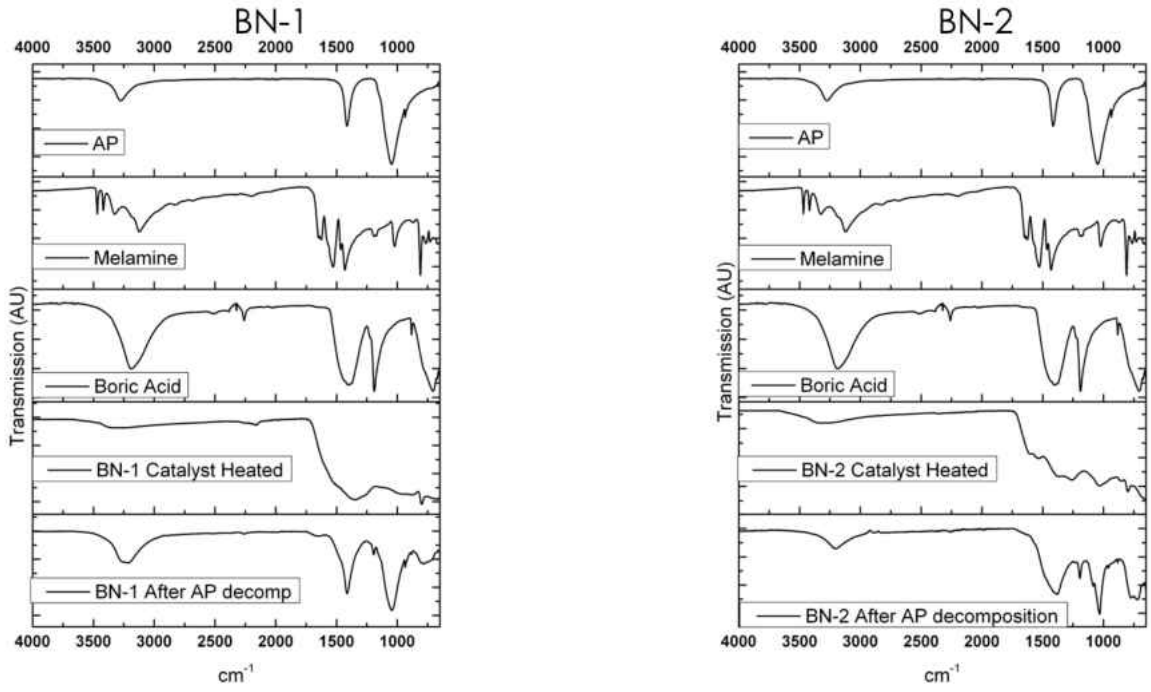

Figure 23:FTIR spectra of the pure catalyst solutions and the residue of the decomposition of 5wt% catalyst solution in AP (Labeled BN-X inAP).

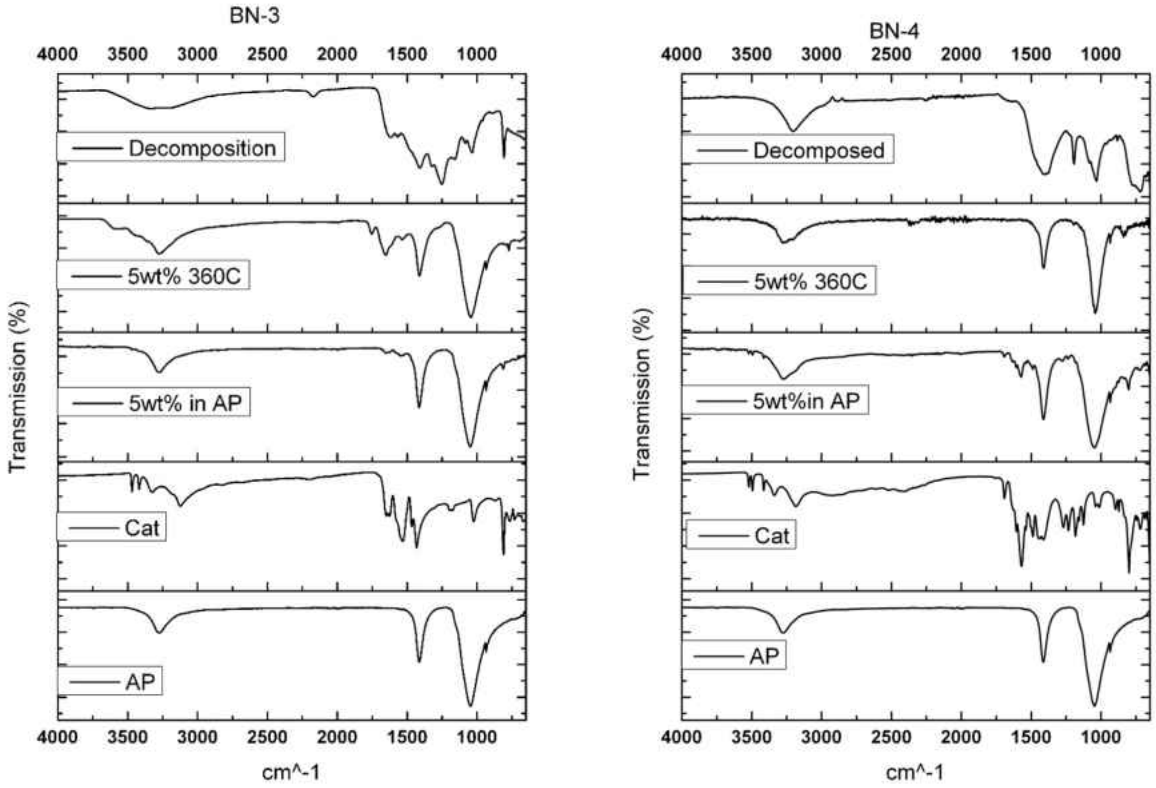

Figure 24: FTIR spectra of the pure catalyst solutions and the residue of the decomposition of 5wt% catalyst solution in AP (Labeled BN-X inAP).

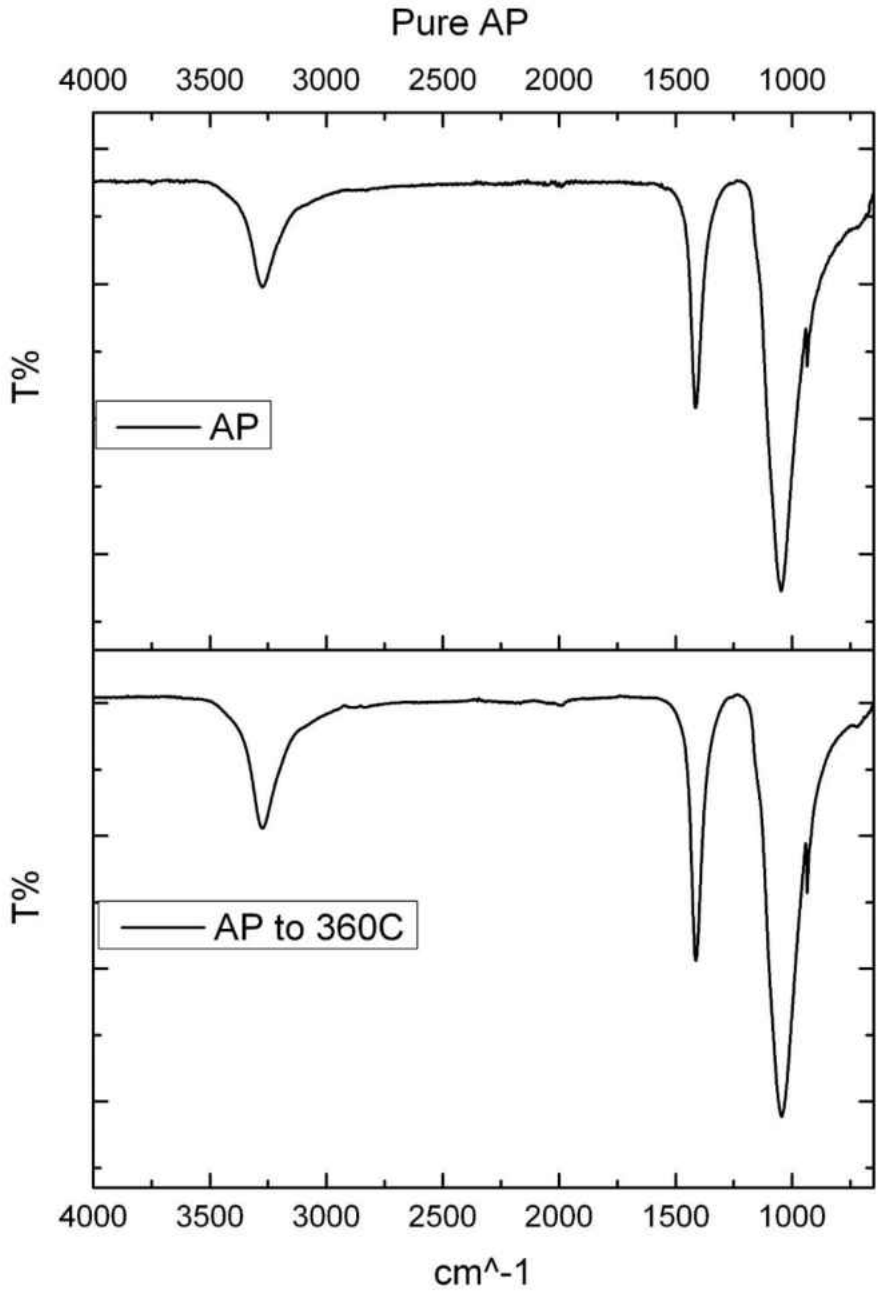

Figure 25: FTIR spectrum of Ammonium Perchlorate salt before decomposition and after being heated to 360°C. No chemical change is seen.

3.2.3 X-Ray Photoelectron Spectroscopy Analysis

XPS analysis was done on the original BN catalyst materials as well as the residue from the decomposition of these material with ammonium perchlorate. It is assumed the ammonium perchlorate decomposes completely leaving no residue. In Figure 25, the XPS survey reaffirms that BN-1 and BN-4 have the same chemical composition while BN-3 is nitrogen-rich and BN-2 is nitrogen-deficient. From the multiplex survey, and deconvolution of the peaks, atomic composition percentage was calculated for each sample before and after decomposition with AP. This is summarized in Table 4. As expected, the BN-3 sample has the most nitrogen, followed by BN-1 and BN-4, while BN-2 has the least amount of nitrogen. Interestingly, BN-1 was seen to have the most boron with 11.2%, followed closely by BN-4 with 9.1, then BN-2 with 6.0% and BN-3 with almost no boron found in the sample with 0.4%. During the decomposition, the catalyst material has unreacted precursor which gets burned off, decreasing the overall weight of the sample, making it seem like the percentage of boron has gone, but in reality the total amount of boron has remained the same. The oxidation of unreacted boron precursor will leave behind solid material, leaving the total amount of boron unchanged In the case of nitrogen species, any unreacted nitrogen precursor will likely form gaseous components, and will leave the sample. This explains the massive loss in nitrogen from the pure catalyst material to the residue of burned material. The nitrogen species may be reacting with the AP and aiding in the decomposition.

Table 4: Atomic composition of BN catalyst materials and residue from burning AP with 5wt% BN catalyst materials

Sample	C%	O%	N%	B%
BN-1	37.8	23.2	27.8	11.2
BN-2	58.8	19.1	16.1	6.0
BN-3	43.9	19.2	45.5	0.4
BN-4	44.8	24.7	21.4	9.1
5wt% BN-1 in AP (600°C)	29	42.1	7.2	21.7
5wt% BN-2 in AP (600°C)	34.8	41.8	5.0	18.5
5wt% BN-3 in AP (600°C)	52.1	23.4	19.0	5.4
5wt% BN-4 in AP (600°C)	47.1	34.9	4.8	13.2

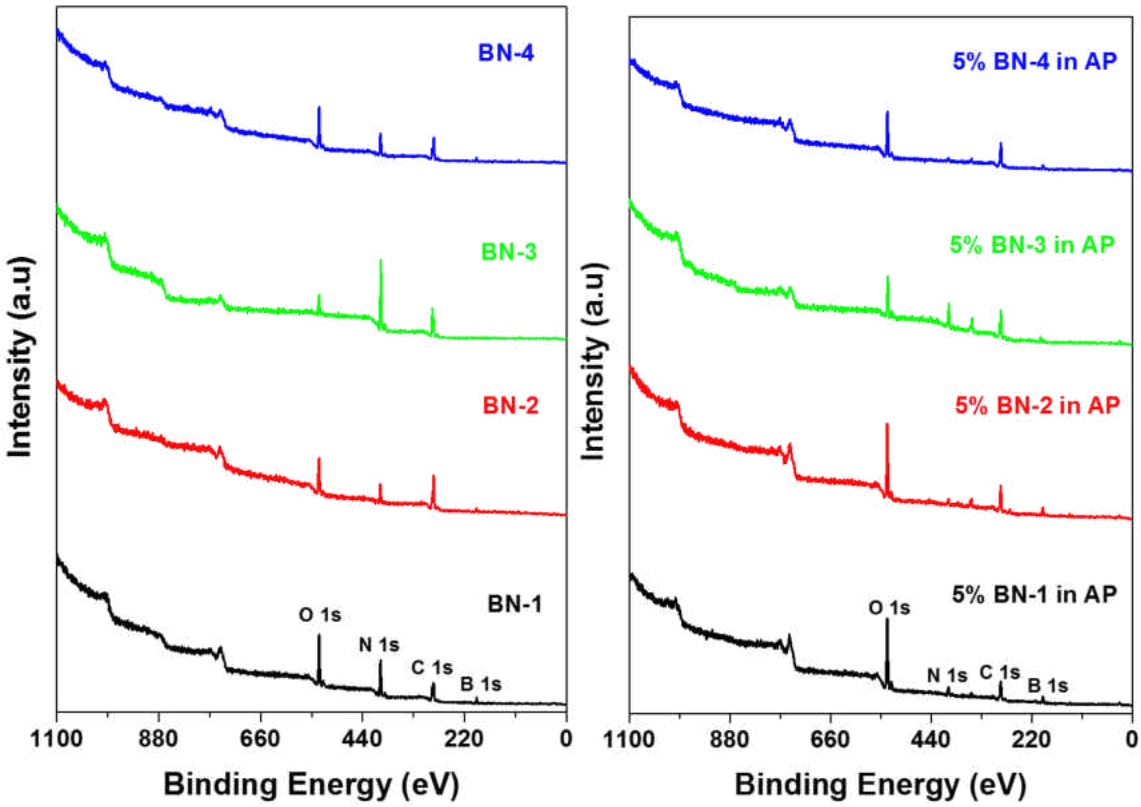

Figure 26: XPS survey of Left) Pure BN catalyst materials and Right)Residue from burning 5wt% BN catalyst material in AP

To examine the specific change in composition of a specific sample from before decomposition to after, we deconvoluted the boron and nitrogen peaks of the catalyst material to examine the specific bonding that's occurring in our sample. When comparing the boron and nitrogen peaks before and after decomposition, we see that before heating the only boron bonding was the B-N bond (Figure 26), and after heating, boron oxides occur from the oxidation of unreacted precursor, as well as the emergence of a boride peak and the maintenance of the original B-N bond (Figure 28). For Nitrogen, originally, we only had the B-N and C-N bond (Figure 27), but after the

reaction (Figure 29) we have the existence of our AP material, suggesting that some AP has adhered to our BN particles, preventing it from fully decomposing, as well as the emergence of nitride peaks, suggesting that the nitrogen species undergo a reaction during the decomposition. It is my belief that the nitrogen species are helping decompose the AP salt by providing an alternative bond between the ammonia and the existing nitrogen species rather than the ionic bond between the ammonia and the perchlorate ion. After this bond substitution, the materials dissociate and decompose into gaseous form.

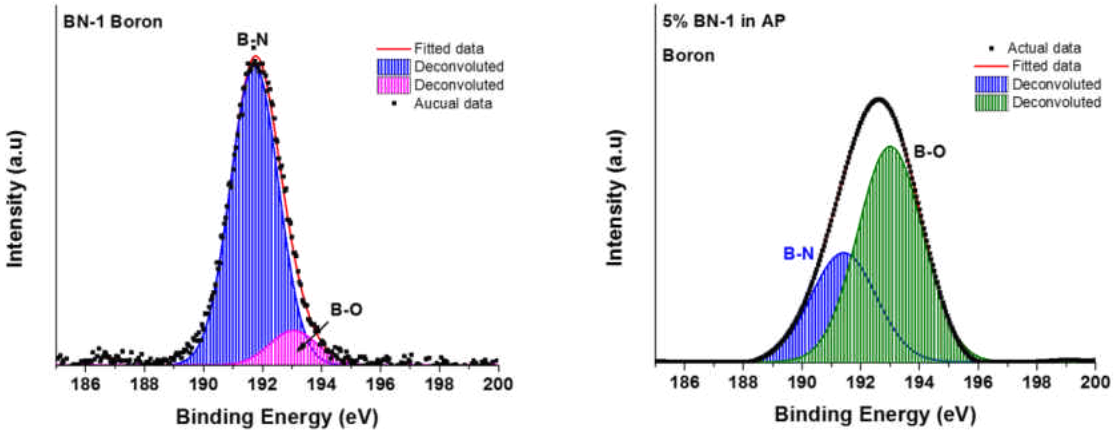

Figure 27: Deconvoluted XPS boron peak from left) pure catalyst and right) residue from decomposition of AP

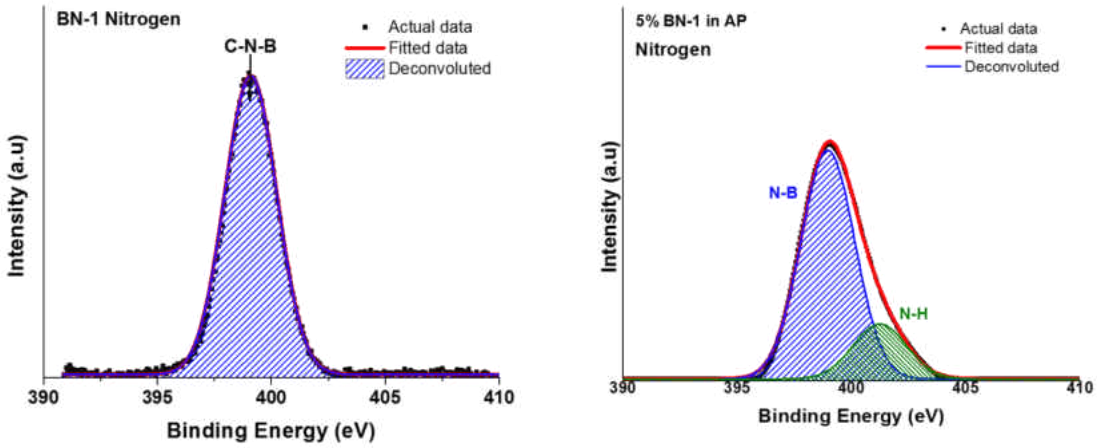

Figure 28: Deconvoluted XPS spectrum of nitrogen peak. left)BN-1 catalyst and right) residue from decomposition of AP

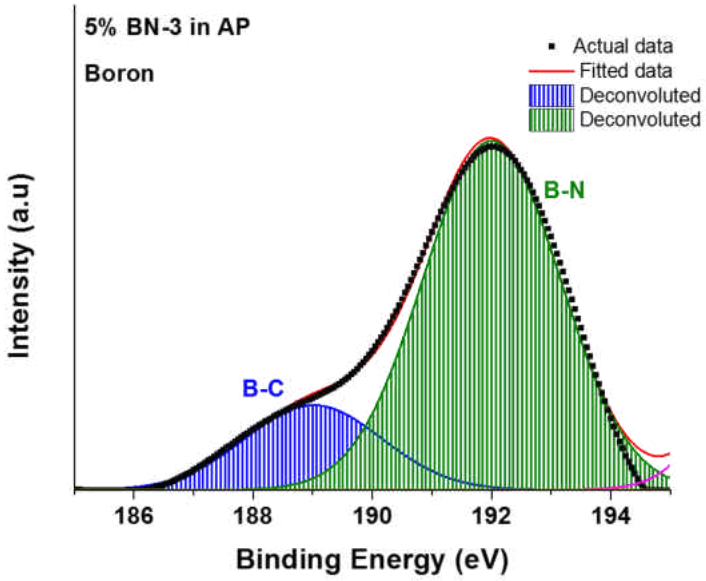

Figure 29: Deconvoluted boron peak for BN-3 after its role in the decomposition of AP

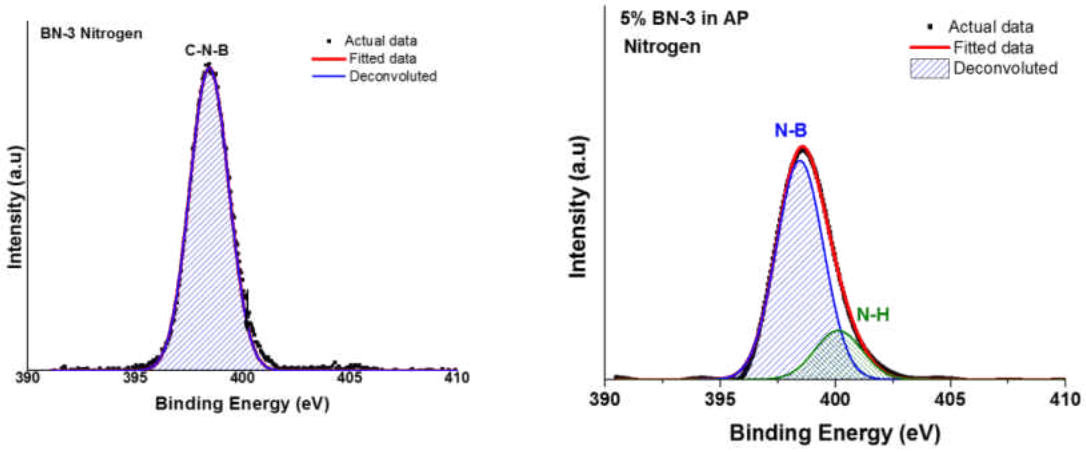

Figure 30: deconvoluted XPS nitrogen spectrum of left) pure BN-3 and right) BN-3 residue after decomposition of 5 wt% BN-3 in AP

CHAPTER FOUR: CONCLUSION

The synthesized BN material has been shown to produce a dramatic change in the decomposition of ammonium perchlorate. Compared to the widely used iron oxide nanoparticles, the BN produces very similar results in terms of heat output, and degree of decomposition during LTD. The AP also shows a lower decomposition activation energy compared to the AP mixed with iron oxide. The BN also has other advantages over the iron oxide nanoparticles such as ease of production, lower molecular weight and cost. The low molecular weight is important when discussion applications of rocketry. A lighter rocket is able to fly farther and faster. The synthesis method makes the BN material cheap to make with very little resources or energy needed.

Amorphous Boron Nitride material was synthesized using a facile hydrothermal method. Variations from the original procedure were also made including boron-rich BN, Nitrogen-rich BN and template free synthesis BN. Full characterization was done on all BN samples and it was shown that the synthesized material contains Carbon and Oxygen as well as Boron and Nitrogen. The existence of oxygen in the samples is most likely due to the samples exposure to atmosphere during synthesis. All samples produced, except the nitrogen-rich sample, were amorphous ribbon-like structures. The nitrogen-rich sample had much larger particles and showed no resemblance to ribbons, but rather stones about 100 microns in size. The lack of crystallinity in the samples was confirmed by SAED and XRD. The relative composition of the samples was measured by XPS and showed that Carbon and Oxygen existed within the material and this was confirmed by EELS spectra. The materials were mixed in AP at a concentration of 5wt% to be studied using DSC/TGA and DRIFTS-FTIR. The DSC/TGA plots showed a dramatic difference in the

decomposition of AP when in the presence of BN samples and Fe_2O_3. The BN catalyst caused the AP to lose up to 77% of its weight during the LTD compared to the 13% weight loss when uncatalyzed. BN-3 caused the highest weight loss in AP, followed by BN-1, BN-4 and then BN-2, which only showed a weight loss of 60.77%. The DSC plot showed a dramatic increase in energy output from the AP during the LTD when catalyzed by BN. BN-3 showed the highest energy output at 13.52 J/g, followed by BN-4, followed by BN-1, and BN-2 showed the smallest energy increase with a heat output of 912 J/g. SEM images of the AP before decomposition and after being heated up to certain temperatures were taken. The AP that was heated in the presence of the catalyst material had a much more porous surface than the uncatalyzed decomposed AP heated up to the same temperatures. SEM images of the residue of the catalyst material were taken and showed a change in the structure of the material. The ribbons underwent a physical change during the heating process as well as a chemical change by reacting with components of the Ammonium Perchlorate salt.

LIST OF REFERENCES

1. Gune, S.G., S. Kulkarni, and S. Panda, *Synergistic hypergolic ignition of solid substituted anilines mixed with magnesium powder and red fuming nitric acid.* Combustion and flame, 1985. **61**(2): p. 189-193.
2. Reid, D.L., et al., *Nanoscale additives tailor energetic materials.* Nano Letters, 2007. **7**(7): p. 2157-2161.
3. Bircumshaw, L. and B.H. Newman, *The thermal decomposition of ammonium perchlorate. I. Introduction, experimental, analysis of gaseous products, and thermal decomposition experiments.* Proceedings of the Royal Society of London. Series A. Mathematical and Physical Sciences, 1954. **227**(1168): p. 115-132.
4. Boldyrev, V., *Thermal decomposition of ammonium perchlorate.* Thermochimica Acta, 2006. **443**(1): p. 1-36.
5. Jacobs, P. and A. Russell-Jones, *On the mechanism of the decomposition of ammonium perchlorate.* AIAA Journal, 1967. **5**(4): p. 829-830.
6. Das, S., et al., *Cerium oxide nanoparticles: applications and prospects in nanomedicine.* Nanomedicine, 2013. **8**(9): p. 1483-1508.
7. Alili, L., et al., *Downregulation of tumor growth and invasion by redox-active nanoparticles.* Antioxidants & redox signaling, 2012.
8. Chaturvedi, S. and P.N. Dave, *A review on the use of nanometals as catalysts for the thermal decomposition of ammonium perchlorate.* Journal of Saudi Chemical Society, 2013. **17**(2): p. 135-149.
9. Hongzhen, D., et al., *Synthesis of Co nanoparticles and their catalytic effect on the decomposition of ammonium perchlorate.* Chinese Journal of Chemical Engineering, 2008. **16**(2): p. 325-328.
10. Jacobs, P.W.M. and H. Whitehead, *Decomposition and combustion of ammonium perchlorate.* Chemical Reviews, 1969. **69**(4): p. 551-590.
11. Kishore, K. and M. Sunitha, *Effect of transition metal oxides on decomposition and deflagration of composite solid propellant systems: a survey.* AIAA Journal, 1979. **17**(10): p. 1118-1125.
12. Patil, K., V. Paiverneker, and S. Jain, *Role of Transition-Metal Fluorides in Ammonium-Perchlorate Decomposition.* Indian Journal of Chemistry-Section A: Inorganic, Physical, Theoretical and Analytical Chemistry, 1978. **16**(2): p. 109-111.
13. Galwey, A. and M. Mohamed, *The low temperature thermal decomposition of ammonium perchlorate: nitryl perchlorate as the reaction intermediate.* Proceedings of the Royal Society of London. A. Mathematical and Physical Sciences, 1984. **396**(1811): p. 425-440.
14. Mosuang, T. and J. Lowther, *Relative stability of cubic and different hexagonal forms of boron nitride.* Journal of Physics and Chemistry of Solids, 2002. **63**(3): p. 363-368.
15. Pakdel, A., Y. Bando, and D. Golberg, *Nano boron nitride flatland.* Chemical Society Reviews, 2014. **43**(3): p. 934-959.
16. Lin, Y., et al., *Defect functionalization of hexagonal boron nitride nanosheets.* The Journal of Physical Chemistry C, 2010. **114**(41): p. 17434-17439.
17. Dean, C., et al., *Boron nitride substrates for high-quality graphene electronics.* Nature nanotechnology, 2010. **5**(10): p. 722-726.
18. Zhi, C., et al., *Large-scale fabrication of boron nitride nanosheets and their utilization in*

polymeric composites with improved thermal and mechanical properties. Advanced Materials, 2009. **21**(28): p. 2889-2893.
19. Feng, L., et al., *The effect of surface microstructures and surface compositions on the wettabilities of flower petals.* Soft Matter, 2011. **7**(6): p. 2977-2980.
20. Zhang, X., et al., *Mechanical properties and ablation behavior of ZrB 2–SiC ceramics fabricated by spark plasma sintering.* International Journal of Refractory Metals and Hard Materials, 2015. **48**: p. 120-125.
21. Li, J., et al., *Activated boron nitride as an effective adsorbent for metal ions and organic pollutants.* Scientific reports, 2013. **3**.
22. Lu, K., W. Wei, and J. Wang, *Grain growth kinetics and interfacial energies in nanocrystalline Ni-P alloys.* Journal of applied physics, 1991. **69**(10): p. 7345-7347.